

Low-Background, High-Efficiency Setup for the Study of $^{22}\text{Ne}(p, \gamma)^{23}\text{Na}$ Reaction at Low Energy

Federico FERRARO^{1,2} on behalf of the LUNA collaboration

¹ *Università degli Studi di Genova, Genova, Italy*

² *INFN - Sezione di Genova, Genova, Italy*

E-mail: federico.ferraro@ge.infn.it

(Received August 20, 2016)

Measuring cross sections of astrophysical interest requires a low-background, high-efficiency setup and a very pure target. The Laboratory for Underground Nuclear Astrophysics (LUNA) developed a dedicated setup for the cross section measurement of the $^{22}\text{Ne}(p, \gamma)^{23}\text{Na}$ reaction. A windowless gas target and a six-fold, optically segmented BGO detector surrounding the interaction volume were used. A calorimetric system was developed for the real-time measurement of the beam current. Three recently measured resonances at 156.2, 189.5 and 259.7 keV and the possible resonances at 71 and 105 keV have been investigated with high statistics. Direct capture measurements were carried out as well.

KEYWORDS: low background, high efficiency, underground physics, nuclear astrophysics, gamma spectroscopy, gas target

1. Introduction

Cross sections in the Gamow window are essential to stellar evolution studies. Depending on the interacting nuclei and temperature, the Gamow window can be in the range of few hundreds of keV or lower, where the cross section drops off very quickly. For such low interaction rates, the cosmic rays induced background often prevents the cross section measurement in surface laboratories, in spite of active background suppression.

LUNA is located in the Gran Sasso National Laboratory (LNGS), Italy. It consists in the world's only deep underground accelerator facility in running conditions, operating a 400 kV high-current electrostatic accelerator [1]. LUNA benefits from a 1400 m thick rock overburden, corresponding to 3800 meter water equivalent (m.w.e.), which shields the LNGS from cosmic muons, suppressing their flux by six orders of magnitude and leading to a very low background [2, 3]. LUNA is provided with two beamlines, respectively equipped with a solid target and a windowless extended gas target. This latter was recently used to study the $^{22}\text{Ne}(p, \gamma)^{23}\text{Na}$ reaction, which belongs to the Neon-Sodium (NeNa) cycle of hydrogen burning and is relevant to red giant branch (RGB) stars, asymptotic giant branch (AGB) stars, classical novae (CN) and supernovae Ia (SN Ia) explosions [4–7]. The NeNa cycle greatly influences the nucleosynthesis of the elements between ^{20}Ne and ^{27}Al since it is linked to the MgAl cycle. According to literature, several low-energy resonances give a relevant contribution to the reaction rate, but some of them have never been directly observed [8].

2. LUNA windowless gas target

The gas target beamline is provided with a system that allows the recycling of the gas, as shown in Fig. 1. A differential pumping system made of three stages makes the gas flow from the target chamber, all the way through a purifier and back to the chamber. The pressure goes from few mbar

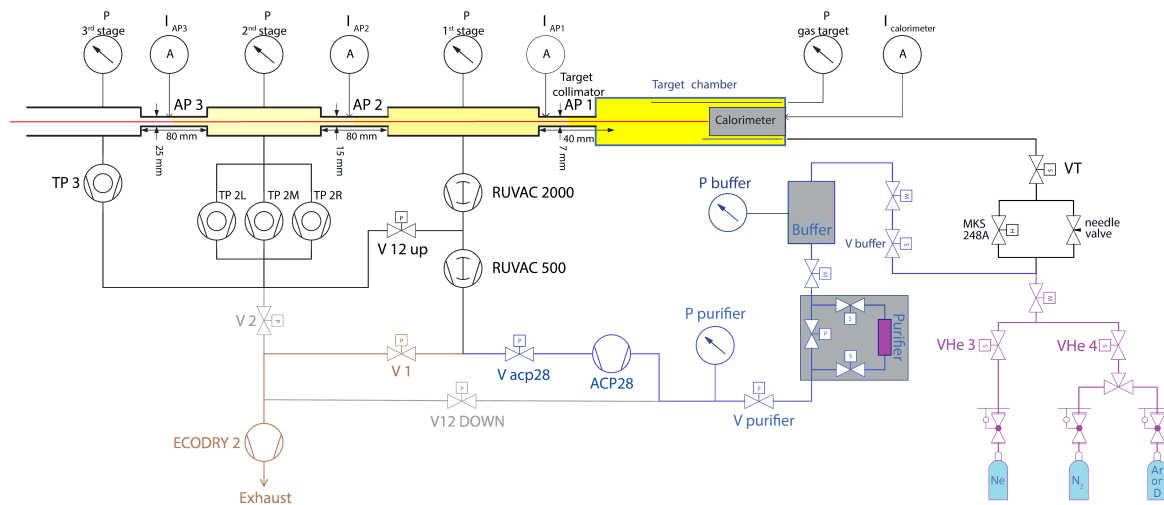


Fig. 1. Beamline pumping system schematic. The beam comes from the left side and goes towards the calorimeter, while the gas enters the target chamber and comes out through aperture AP1. Most of the gas flows through the RUVAC pumps of the first pumping stage.

in the target chamber down to 10^{-7} mbar in the third pumping stage (the one which is closer to the accelerator). The purifier reduces the impurity levels for H_2O , O_2 , H_2 , CO , CO_2 , CH_4 and N_2 , which otherwise would increase the beam-induced background. Recycling permits not to lose the enriched gas, while the chemical getter guarantees the purification from possible contaminants coming from the pumping system itself. The beam comes out of the accelerator, goes through the apertures between the pumping stages and impinges on the calorimeter after crossing the interaction chamber, which is 10.8 cm long and is provided with a water-cooled 4 cm long collimator. A similar setup was used for the previous phase of the experiment, which used different target chamber and detectors [8–10].

A copy of the interaction chamber, provided with tubes and flanges, was used to measure the gas pressure and temperature along the beam direction in different positions and obtain the density profile without the beam. The effect of the beam on the Ne gas target was already studied and the beam-heating correction has to be applied. The calorimeter consists in a heat-conductive device with two sides at different temperature and is able to operate up to 200 W. A feedback is realized with NI-cRIO modules and a LabVIEW software, together with four Resistive Temperature Detectors (RTDs) and a remotely controlled power supply. The feedback system delivers power to the heaters of the hot side (which is also the beam stop) in such a way it is always kept at 70 °C, while the cold side (the one which is not exposed to the beam) is kept at about 7 °C by a chiller. As a result, a constant power is needed to keep the hot side at 70 °C, and the total power delivered to the beam stop is then the sum of two contributions: beam power and heaters' one. Heaters' power is measured and logged every second, allowing the assessment of the beam contribution. The beam current is then obtained dividing the beam power by the energy of the protons in front of the beam stop (in eV), taking into account the initial beam energy and the energy loss inside the target.

A 6-fold, optically segmented Bismuth Germanium Oxide (BGO) detector was used. To achieve the highest detection efficiency the detector surrounds almost completely the interaction chamber. The detector provides a coverage close to 4π and the efficiency reaches 70%, depending on the photon energy. Each segment of the detector is provided with an independent acquisition chain, involving the crystal, the photo-multiplier tube, a pre-amplifier and a digitizer. Data from each event are digitized and stored for each segment, including energy and time stamp. Offline coincidence analysis is possible, allowing for the production of the single segment spectra and the reconstruction of the sum spectrum, where the peak close to the reaction Q-value is visible.

3. Experiment

Below 2.6 MeV natural and intrinsic background dominate the spectrum, both with or without beam, with a higher energy tail due to the sum of background events. Above 5 MeV, beam-off spectra are quite clean and most of the background is induced by the beam, due to ^{11}B , ^{18}O , ^{19}F and ^2H residuals, depending on the beam energy. Some counts between 5 and 10 MeV are caused by thermal neutron captures on Fe nuclei in surrounding steel-made objects. Few counts above 10 MeV are caused by cosmic radiation.

We observed a decrease of ^{11}B and ^{19}F levels after cleaning the interaction chamber and the collimator in two ultrasonic bath, at first using a cleaning agent and then citric acid. The same pieces, together with the calorimeter, have been rinsed many times with deionized water. Despite the cleaning, the contamination did not vanish completely, but we managed to reduce it, obtaining a reasonably low background in the region of interest for the $^{22}\text{Ne}(p, \gamma)^{23}\text{Na}$ reaction, around 9 MeV.

The efficiency was measured by means of radioactive sources (^7Be , ^{137}Cs , ^{60}Co and ^{88}Y) and the well known $^{14}\text{N}(p, \gamma)^{15}\text{O}$ resonance at $E_p^{res} = 278$ keV, populated in different positions inside the chamber. The peaks from ^{40}K , ^{207}Bi and ^{208}Tl were used for the energy calibration, together with the peaks originating from ^{15}O excited states decay.

As a crosscheck we measured the strength of the resonances at $E_p^{res} = 156.2$, 189.5 and 259.7 KeV. High statistics was collected around the tentative resonances at 71 keV and 105 keV. Data on direct capture were taken as well and the ^{22}Ne peak at $Q + E_{cm}$ clearly emerges from the background. The analysis is in progress and the results will be published soon.

References

- [1] A. Formicola, G. Imbriani, M. Junker, D. Bemmerer, R. Bonetti, C. Brogгинi, C. Casella, P. Corvisiero, H. Costantini, G. Gervino, C. Gustavino, A. Lemut, P. Prati, V. Roca, C. Rolfs, M. Romano, D. Schürmann, F. Strieder, F. Terrasi, H.-P. Trautvetter, S. Zavatarelli, Nucl. Instrum. Methods Phys. Res., Sect. A **507**, (2003) 609
- [2] H. Costantini, A. Formicola, G. Imbriani, M. Junker, C. Rolfs and F. Strieder, Rep. Prog. Phys. **72**, (2009) 086301
- [3] C. Brogгинi, D. Bemmerer, A. Guglielmetti and R. Menegazzo, Ann. Rev. Nucl. Sci. **60**, (2010)
- [4] J. Marion and W. Fowler, Astrophys. J. **125**, (1957) 221
- [5] C. Iliadis, A. Champagne, J. José, S. Starrfield, and P. Tupper, Astrophys. J. Suppl. Ser. **142**, (2002) 105
- [6] A. Boeltzig, C. G. Bruno, F. Cavanna, S. Cristallo, T. Davinson, R. Depalo, R. J. deBoer, A. Di Leva, F. Ferraro, G. Imbriani, P. Marigo, F. Terrasi, M. Wiescher, Eur. Phys. J. A **52** (2016) 75
- [7] R. Depalo, F. Cavanna, F. Ferraro, A. Slemmer, T. Al-Abdullah, S. Akhmalaliev, M. Anders, D. Bemmerer, Z. Elekes, G. Mattei, S. Reinicke, K. Schmidt, C. Scian, and L. Wagner, Phys Rev. C **92** (2015) 045807
- [8] F. Cavanna, R. Depalo, M. Aliotta, M. Anders, D. Bemmerer, A. Best, A. Boeltzig, C. Broggini, C.G. Bruno, A. Caciolli, P. Corvisiero, T. Davinson, A. di Leva, Z. Elekes, F. Ferraro, A. Formicola, Zs. Fülöp, G. Gervino, A. Guglielmetti, C. Gustavino, Gy. Gyürky, G. Imbriani, M. Junker, R. Menegazzo, V. Mossa, F.R. Pantaleo, P. Prati, D.A. Scott, E. Somorjai, O. Straniero, F. Strieder, T. Szücs, M.P. Takács, and D. Trezzi, Phys. Rev. Lett. **115**, (2015) 252501
- [9] F. Cavanna, R. Depalo, M.-L. Menzel, M. Aliotta, M. Anders, D. Bemmerer, C. Broggini, C. G. Bruno, A. Caciolli, P. Corvisiero, T. Davinson, A. di Leva, Z. Elekes, F. Ferraro, A. Formicola, Zs. Fülöp, G. Gervino, A. Guglielmetti, C. Gustavino, Gy. Gyürky, G. Imbriani, M. Junker, R. Menegazzo, P. Prati, C. Rossi Alvarez, D. A. Scott, E. Somorjai, O. Straniero, F. Strieder, T. Szücs and D. Trezzi, Eur. Phys. J. A **50**, (2014) 179
- [10] R. Depalo, F. Cavanna, M. Aliotta, M. Anders, D. Bemmerer, A. Best, A. Boeltzig, C. Broggini, C. G. Bruno, A. Caciolli, G. F. Ciani, P. Corvisiero, T. Davinson, A. Di Leva, Z. Elekes, F. Ferraro, A. Formicola, Zs. Fülöp, G. Gervino, A. Guglielmetti, C. Gustavino, Gy. Gyürky, G. Imbriani, M. Junker, R. Menegazzo, V. Mossa, F. R. Pantaleo, D. Piatti, P. Prati, O. Straniero, T. Szücs, M. P. Takcs, and D. Trezzi, Phys Rev. C **94**, (2016) 055804